# Fibroblast Growth Factor Receptor Two (FGFR2) Regulates Uterine Epithelial Integrity and Fertility in Mice

Justyna Filant,[2] Franco J. DeMayo,[3] James K. Pru,[2] John P. Lydon,[3] and Thomas E. Spencer[1,2]

[2]Center for Reproductive Biology, Department of Animal Sciences, Washington State University, Pullman, Washington
[3]Molecular and Cell Biology, Baylor College of Medicine, Houston, Texas

## ABSTRACT

Fibroblast growth factors (FGFs) and their receptors (FGFRs) regulate luminal epithelial (LE) cell proliferation in the adult mouse uterus. This study tested the hypothesis that FGFR2 has a biological role in postnatal development and function of the uterus by conditionally deleting *Fgfr2* after birth using progesterone receptor (*Pgr*)-Cre mice. Adult *Fgfr2* mutant female mice were initially subfertile and became infertile with increasing parity. No defects in uterine gland development were observed in conditional *Fgfr2* mutant mice. In the adult, *Fgfr2* mutant mice possessed a histologically normal reproductive tract with the exception of the uterus. The LE of the *Fgfr2* mutant uterus was stratified, but no obvious histological differences were observed in the glandular epithelium, stroma, or myometrium. Within the stratified LE, cuboidal basal cells were present and positive for basal cell markers (KRT14 and TRP63). Nulliparous bred *Fgfr2* mutants contained normal numbers of blastocysts on Day 3.5 postmating, but the number of embryo implantation sites was substantially reduced on Day 5.5 postmating. These results support the idea that loss of FGFR2 in the uterus after birth alters its development, resulting in LE stratification and peri-implantation pregnancy loss.

*endometrium, female reproductive tract, implantation, mice, rodents, uterus*

## INTRODUCTION

Development, growth, and adult function of the uterus and many other epitheliomesenchymal organs are governed by epithelial-stromal interactions that regulate morphogenetically and physiologically important cell behaviors including proliferation, migration, and differentiation [1–3]. Tissue recombination studies in rodents clearly indicate that uterine mesenchyme/stroma directs and specifies patterns of epithelial development and function, whereas the epithelium is required to support the organization of uterine mesenchyme and myometrial differentiation [1, 2, 4–6]. In mice, distinct cytodifferentiation of the uterine mesenchyme into endometrial stroma and myometrium is complete by 2 wk after birth. In addition, the glandular epithelium (GE) develops from the luminal epithelium (LE) beginning on Postnatal Day 7 (PD 7), and the uterus is histoarchitecturally mature by 30 days after birth [6–8].

Communication between different cell types within epitheliomesenchymal organs is mediated by paracrine, autocrine, and juxtacrine pathways. In the developing neonatal uterus, epithelial-stromal interactions are mediated by *Wnt* proteins, intrinsic growth factors, and likely changes in the composition and distribution of the extracellular matrix [1, 9–12]. In the adult uterus, endometrial proliferation and differentiation are regulated by the ovarian steroid hormones, estrogen and progesterone [13]. Under the influence of these steroids, the LE, GE, and stroma express genes important for blastocyst implantation, including cytokines, lipid mediators, enzymes, transporters, and growth factors (for a review, see [14, 15]). Fibroblast growth factors (FGFs) and their receptors regulate epithelial cell proliferation, migration, and differentiation in many epitheliomesenchymal organs, including the lung, mammary gland, prostate, and kidney [16–20]. Components of the FGF signaling pathway are expressed in the uterus and may act as paracrine and/or autocrine mediators of epithelial-stromal interactions [9, 21]. For example, *Fgf7* is expressed in the stroma of the mouse uterus, and treatment of neonatal mice with FGF7 stimulated proliferation of the uterine epithelium [22]. In the adult mouse, progesterone inhibits expression of several *Fgfs* (*Fgf1, Fgf2, Fgf9, Fgf18*) in the stroma, which is key for progesterone inhibition of estrogen-stimulated LE cell proliferation in the uterus [9]. The FGFs can bind to extracellular domains of IIIb or IIIc isoforms of FGF receptor (FGFR) 2 as well as FGFR 1, 3, or 4 (for a review, see [23]). In many organs, FGFR2IIIb is expressed primarily in epithelia and is activated by FGF 1, 3, 7, and 10, which are produced mainly by the mesenchyme; in contrast, FGFR2IIIc is expressed predominantly in the mesenchyme and is activated by FGF 2, 4, 6, 8, and 9 [24–27]. Both FGFR2IIIb and FGFR2IIIc are present in the uterine epithelia but not stroma of PD 15 neonatal mice [21]. In the adult mouse uterus, immunoreactive FGFR2 was detected in both epithelial and stromal compartments of adult mouse uterus [9].

Collectively, available results support the hypothesis that FGFR2 and its ligands have a biological role in postnatal development and function of the mouse uterus. The definitive role of FGFR2 in postnatal uterine development and function requires a conditional knockout, because global deletion of this gene in the embryo results in embryonic lethality [28]. Therefore, we conditionally ablated *Fgfr2* immediately after birth in the uterus using *Fgfr2flox* and *PgrCre* mice to test our hypothesis. The conditional ablation of *Fgfr2* after birth resulted in progressive stratification of the LE in the uterus and pregnancy loss in the adult.

## MATERIALS AND METHODS

### Generation of Fgfr2 Conditional Mutant Females

All the animal procedures were approved by the Institutional Animal Care and Use Committee of Washington State University and conducted according to the Guide for the Care and Use of Laboratory Animals and institutional guidelines. The B6.129-*Pgrtm2 (cre)Lyd* (also known as *PgrCre*) mice have been described [29]. The B6.129X1 (Cg)-*Fgfr2tm1Dor* (termed *Fgfr2f*) mice have a
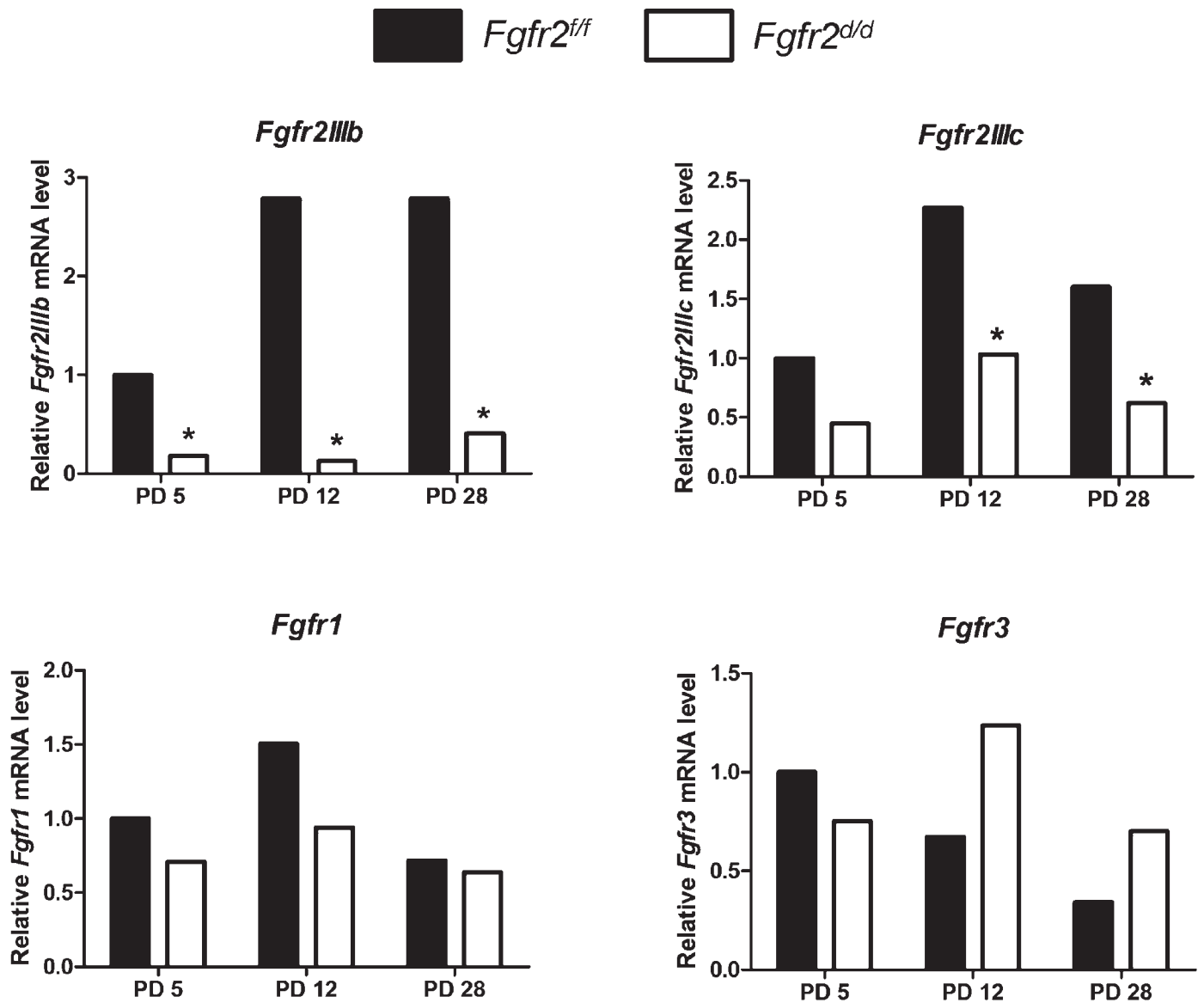
FIG. 1. Expression of *Fgfr* in the uterus of *Fgfr2^{f/f}* and *Fgfr2^{d/d}* mice. The relative level of *Fgfr* mRNA was measured in the uterus by real-time qPCR. Data are presented as fold change relative to the mRNA level on PD 5 in uteri of control mice (n = 4 mice/day/genotype). The asterisk denotes a difference (*P* < 0.05) in mRNA levels within a day.

mutation in which exons 7 through 10 were flanked by a single loxP site in intron 6 and an FRT-flanked neo cassette with a 3′ loxP site in intron 10 [30]. Genotyping was conducted using PCR analysis of DNA extracts from tail biopsies. Briefly, genomic DNA was extracted from the tail biopsies via digestion in 250 µl of 1 M NaOH for 45 min at 95°C. Following incubation, 250 µl of 0.05 M Tris-HCl was added to each tube, and samples were vortexed and centrifuged (16 000 × *g*) for 3 min. Digested material containing genomic DNA (~3 µl) was combined with primer mix, dNTP MIX (2.5 mM each; TaKaRa Bio Inc.), 10× ExTaq Buffer (TaKaRa Bio Inc.), and TaKaRa Ex Taq (TaKaRa Bio Inc.). Primers P1, P2, and P3 (P1: 5′-ATG TTT AGC TGG CCC AAA TG-3′; P2: 5′-TAT ACC GAT CTC CCT GGA CG-3′; P3: 5′-CCC AAA GAG ACA CCA GGA AG-3′) were used to amplify the *Pgr* wild-type (285 bp) and *Cre* (590 bp) alleles. To detect the *Fgfr2* flox allele, primers F1 and F2 (F1: 5′-GTC AAT TCT AAG CCA CTG TCT GCC-3′; F2: 5′-CTC CAC TGA TTA CAT CTA AAG AGC-3′) were designed to amplify the fragments from the wild-type (142 bp) and floxed (207 bp) alleles. PCR reactions were carried out for 35 cycles of 95°C for 45 sec, 61°C (*Pgr*) or 59°C (*Fgfr2*) for 1 min, and 72°C for 1 min.

Postnatal samples were obtained after parturition, and the day that pups were born was considered PD 0. To study pregnancy, *Fgfr2* control females (*Pgr^{+/+};Fgfr2^{f/f}* termed *Fgfr2^{f/f}*) and conditional *Fgfr2* mutant females (*Pgr^{Cre/+};Fgfr2^{f/f}* termed *Fgfr2^{d/d}*) were mated with fertile males, and the day

of postcoital vaginal plug was designated as Gestational Day 0.5 (GD 0.5). On GD 5.5, implantation sites were visualized by injection of 1% Evans blue dye (Sigma-Aldrich) into the tail vein 5 min before necropsy. At the time of necropsy, the uterine horns were fixed in 4% paraformaldehyde in PBS (pH 7.2) overnight and paraffin embedded for histology or frozen in liquid nitrogen at stored at −80°C for RNA extraction and analysis.

### RNA Isolation and Quantitative Real-Time RT-PCR Analysis

Gene expression analysis via quantitative real-time PCR (qPCR) was conducted using methods previously described by our laboratory [31]. Briefly, total RNA was isolated from uterine samples using TRIzol reagent (Invitrogen) according to the manufacturer's recommendations. Genomic DNA was digested with DNase I followed by RNA cleanup using Qiagen RNeasy MinElute (Qiagen). Total RNA (1 µg) was reverse transcribed using iScript Reverse Transcription Supermix for RT-qPCR (Bio-Rad Laboratories). Control reactions in the absence of reverse transcriptase were prepared for each sample to test for genomic DNA contamination. Real-time PCR analysis was performed using CFX Connect Real-Time PCR Detection System (Bio-Rad) and SsoAdvanced SYBR Green Supermix (Bio-Rad) that uses specific oligonucleotide primers designed by Oligo 7 program (Molecular Biology Insights, Inc.) (see Supplemental Table S1, available online at www.biolreprod.
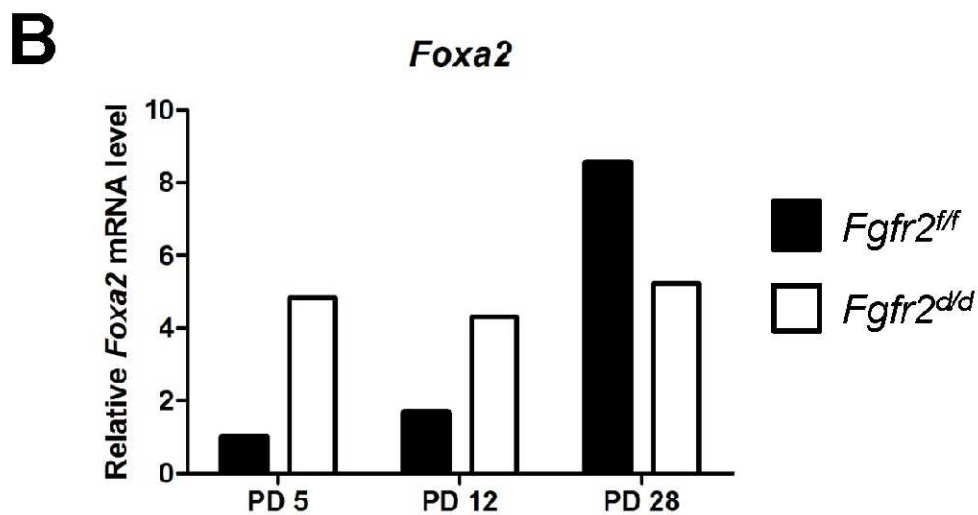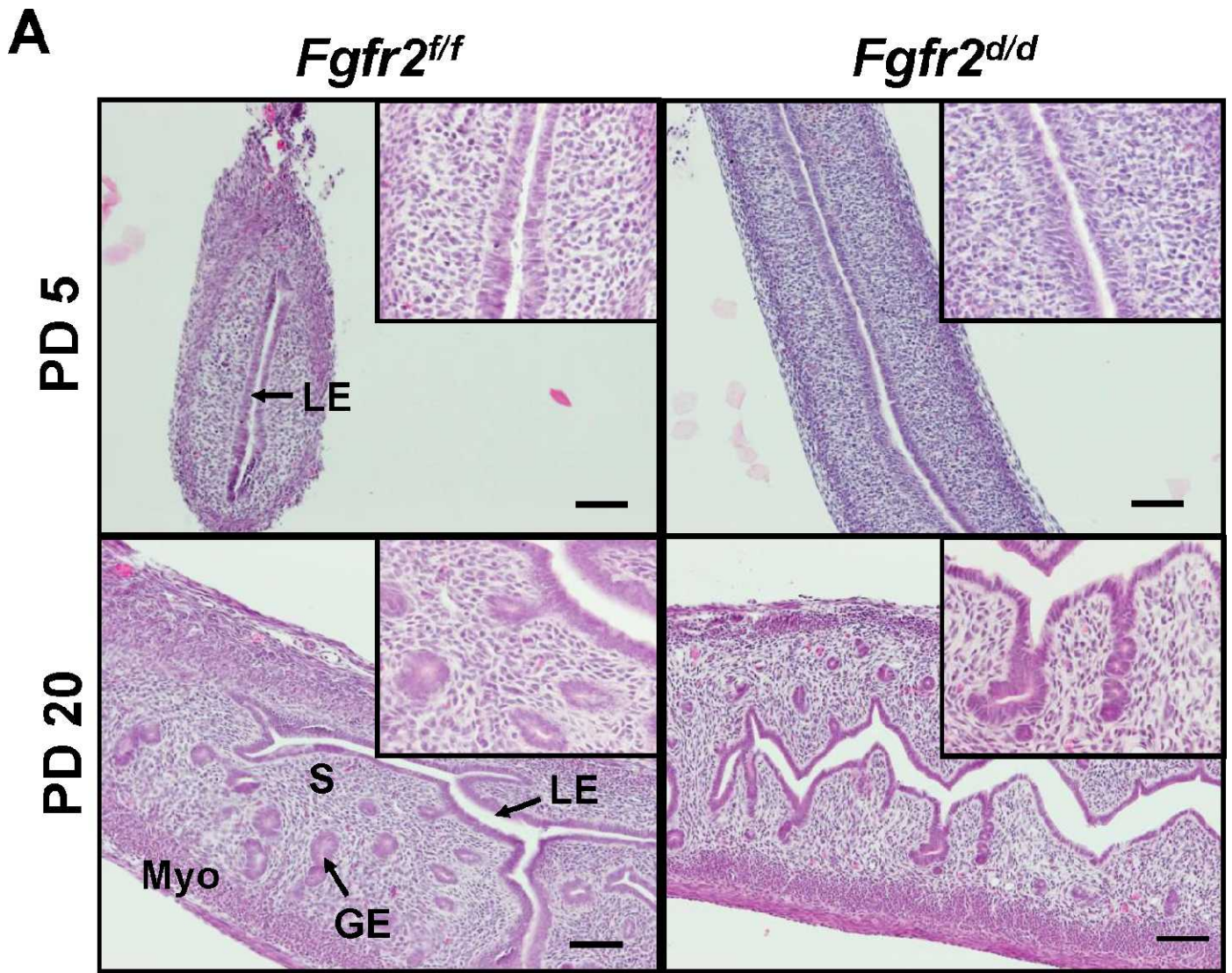
**A**



**B**



FIG. 2. Postnatal conditional ablation of *Fgfr2* has no effect on development of the uterus after birth. **A**) Histoarchitecture of the neonatal uterus in *Fgfr2^f/f* and *Fgfr2^d/d* mice. Sections of the neonatal uterus were stained with hematoxylin and eosin. No differences in histoarchitecture of the uterus were observed between *Fgfr2^f/f* and *Fgfr2^d/d* mice. LE, luminal epithelium; GE, glandular epithelium; Myo, myometrium; PD, postnatal day; S, stroma. Bar = 100 μm. **B**) Expression of *Foxa2* in the neonatal uterus of *Fgfr2^f/f* and *Fgfr2^d/d* mice. The relative level of *Foxa2* mRNA was measured in the uterus by real-time qPCR. Data are presented as fold change relative to the mRNA level on PD 5 in uteri of control mice (n = 4 mice/day/genotype).

TABLE 1. *Fgfr2$^{d/d}$* mutant mice are subfertile.

| Female genotype | No. of females | No. of pups | No. of litters | Average pups per litter | Average litters per female |
|---|---|---|---|---|---|
| *Fgfr2$^{f/f}$* | 6 | 206 | 32 | 6.4 ± 0.7 | 5.3 ± 0.5 |
| *Fgfr2$^{d/d}$* | 10 | 62* | 24* | 2.6 ± 0.6* | 2.4 ± 0.6* |

* Effect of genotype ($P < 0.01$).

org). Expression of *Fgfr2IIIb, Fgfr2IIIc,* and *Foxa2* mRNA were analyzed using TaqMan Gene Expression Assays (Applied Biosystems). Mouse *Rpl13a* was used as a reference gene.

### Immunohistochemistry

Uteri were fixed in 4% paraformaldehyde, embedded in paraffin, and sectioned at 5 μm. Sections were mounted on slides, deparaffinized, and rehydrated in a graded alcohol series. Uterine sections were subjected to antigen retrieval by boiling in 10 mM citrate buffer (pH 6.0) for 10 min, preincubated in 10% normal goat serum in PBS (pH 7.5) for 10 min at room temperature, and then incubated overnight in primary antibody at 4°C. The following primary antibodies, diluted in 1% bovine serum albumin in PBS (pH 7.5), were used: anti-FOXA2 at 1.2 μg/ml (LS-C 138006; LifeSpan Biosciences); anti-PTGS2 at 2 μg/ml (160106; Cayman Chemicals); anti-KRT14 at 2 μg/ml (LS-B3916; Lifespan Biosciences); or anti-TRP63 at 1 μg/ml (4981; Cell Signaling). Negative controls were conducted by substituting the primary antibody with normal rabbit immunoglobulin G (2027; Santa Cruz Biotechnology) at the same final concentration. Sections were washed in PBS and incubated with 5 μg/ml biotinylated secondary antibody (PK-6101; Vector Laboratories) followed by immunoreactive protein visualization using a Vectastain Elite ABC kit (Vector Laboratories) and diaminobenzidine tetrahydrochloride (Sigma-Aldrich) as the chromagen. Sections were counterstained with hematoxylin before affixing the coverslips.

### Statistical Analyses

All the quantitative data were subjected to least-squares analyses of variance using the General Linear Models procedures of the Statistical Analysis System (SAS Institute Inc.). In all the analyses, error terms used in tests of significance were identified according to the expectation of the mean squares for error. Significance ($P < 0.05$) was determined by probability differences of least-squares means. Litter size data were analyzed for effects of genotype (*Fgfr2$^{f/f}$* or *Fgfr2$^{d/d}$*), parity, and their interaction. For analysis of real-time PCR data from neonatal mice, the Ct values of the target mRNA were analyzed for effects of genotype, day, and their interaction with the *Rpl13a* or *Rn18s* used as a covariate. Real-time PCR data are presented as fold change relative to the mRNA level in uteri from control *Fgfr2$^{f/f}$* mice.

## RESULTS

### Generation of Mice with Conditional Inactivation of Fgfr2 in the Uterus

Global deletion of *Fgfr2*, which encompasses both isoforms (*IIIb* and *IIIc*), results in early embryonic lethality [28]. Null *Fgfr2IIIb* mice exhibit perinatal lethality, with limb, submaxillary gland, and lung agenesis [17, 32]. In contrast, mice homozygous for the *Fgfr2IIIc* mutation are viable and fertile, likely due to functional compensation by *Fgfr2IIIb* [33]. Thus, conditional ablation of both *Fgfr2IIIb* and *Fgfr2IIIc* in the uterus was conducted by crossing *Pgr$^{Cre}$* mice with *Fgfr2$^{flox}$* (*Fgr2$^{f/f}$*) mice to generate *Pgr$^{Cre/+}$;Fgfr2$^{f/f}$* (termed *Fgfr2$^{d/d}$*). In all the analyses, *Pgr$^{+/+}$;Fgfr2$^{f/f}$* (also known as *Fgfr2$^{f/f}$*) female mice were used as the control. The Cre excision activity in the *Pgr$^{Cre}$* mouse model is restricted to cells that express the PGR after birth, including the uterus, ovary, oviduct, pituitary gland, and mammary gland [29]. Expression of *Pgr* is initiated in the reproductive tract only after birth, and PGR is present in the uterine LE by PD 3 and in the stroma by PD 6 [6, 34].

To assess the efficiency of ablation, expression of *Fgfr2IIIb* and *Fgfr2IIIc* was examined in the developing neonatal uterus (Fig. 1). Expression of both *Fgfr2* isoforms was attenuated in

the uterus of neonatal *Fgfr2$^{d/d}$* mice (Fig. 1). Relative levels of *Fgfr2IIIb* mRNA increased (genotype × day, $P < 0.01$) in the uterus of *Fgfr2$^{f/f}$* but not *Fgfr2$^{d/d}$* mice after birth. Similarly, relative levels of *Fgfr2IIIc* mRNA increased (day, $P < 0.05$) in the uterus of *Fgfr2$^{f/f}$* mice after birth, but the levels of *Fgfr2IIIc* mRNA were lower (genotype, $P < 0.01$) in mutant mice. Both *Fgfr1* and *Fgfr3* are also expressed in mouse uterus [9, 21]; however, *Fgfr1* or *Fgfr3* expression was not different ($P > 0.10$) in uteri of *Fgfr2$^{f/f}$* and *Fgfr2$^{d/d}$* neonatal mice (Fig. 1).

Examination of the female reproductive tract from *Fgfr2$^{f/f}$* and *Fgfr2$^{d/d}$* mice revealed no obvious morphological or histoarchitectural differences in the uterus on PD 5 and PD 20 (Fig. 2A). Histological analysis revealed no differences in the development of endometrial glands in the uterus of *Fgfr2$^{d/d}$* as compared with *Fgfr2$^{f/f}$* mice after birth. In the neonatal and adult uterus, forkhead transcription factor box A2 (FOXA2) is expressed solely in GE and is an essential transcription factor governing endometrial gland differentiation and development in the neonatal mouse uterus [31, 35–37]. Interestingly, relative levels of *Foxa2* mRNA were higher (day × genotype, $P < 0.05$) in the uteri of *Fgfr2$^{d/d}$* than *Fgfr2$^{f/f}$* mice on PD 5 and 12, but not on PD 28 (Fig. 2B).

### Conditional Deletion of Fgfr2 Impairs Female Fertility

To determine the effect of conditional deletion of *Fgfr2* on female fertility, *Fgfr2$^{f/f}$* and *Fgfr2$^{d/d}$* mice were bred to wild-type male mice of proven fertility. In a 6-mo breeding trial, *Fgfr2$^{f/f}$* mice exhibited normal fecundity, whereas the *Fgfr2$^{d/d}$* mice displayed severe subfertility (Table 1). The number of pups per litter and litters per female were greater ($P < 0.01$) in
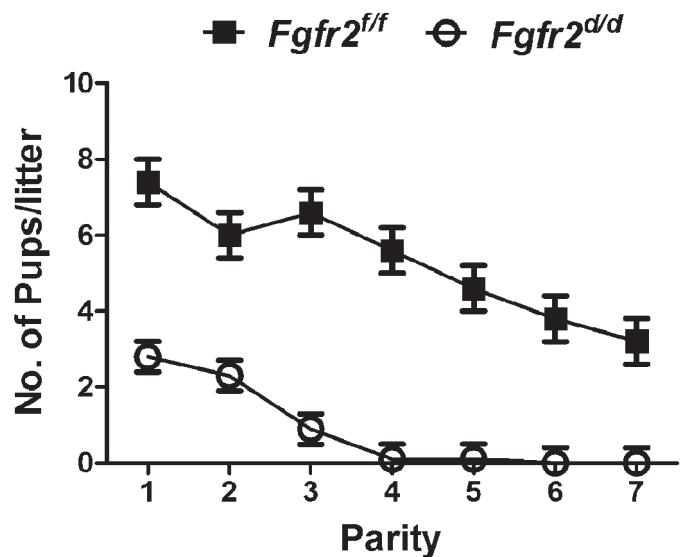


FIG. 3. Effect of conditional ablation of *Fgfr2* in the uterus on female fertility. The number of pups per litter is presented (least-square mean ± SE) by parity for adult *Fgfr2$^{f/f}$* (n = 6) and *Fgfr2$^{d/d}$* (n = 10) female mice mated with fertile males. Note the subfertility present in the primiparous mutant mice that transitions to complete infertility (genotype × parity, $P < 0.05$).
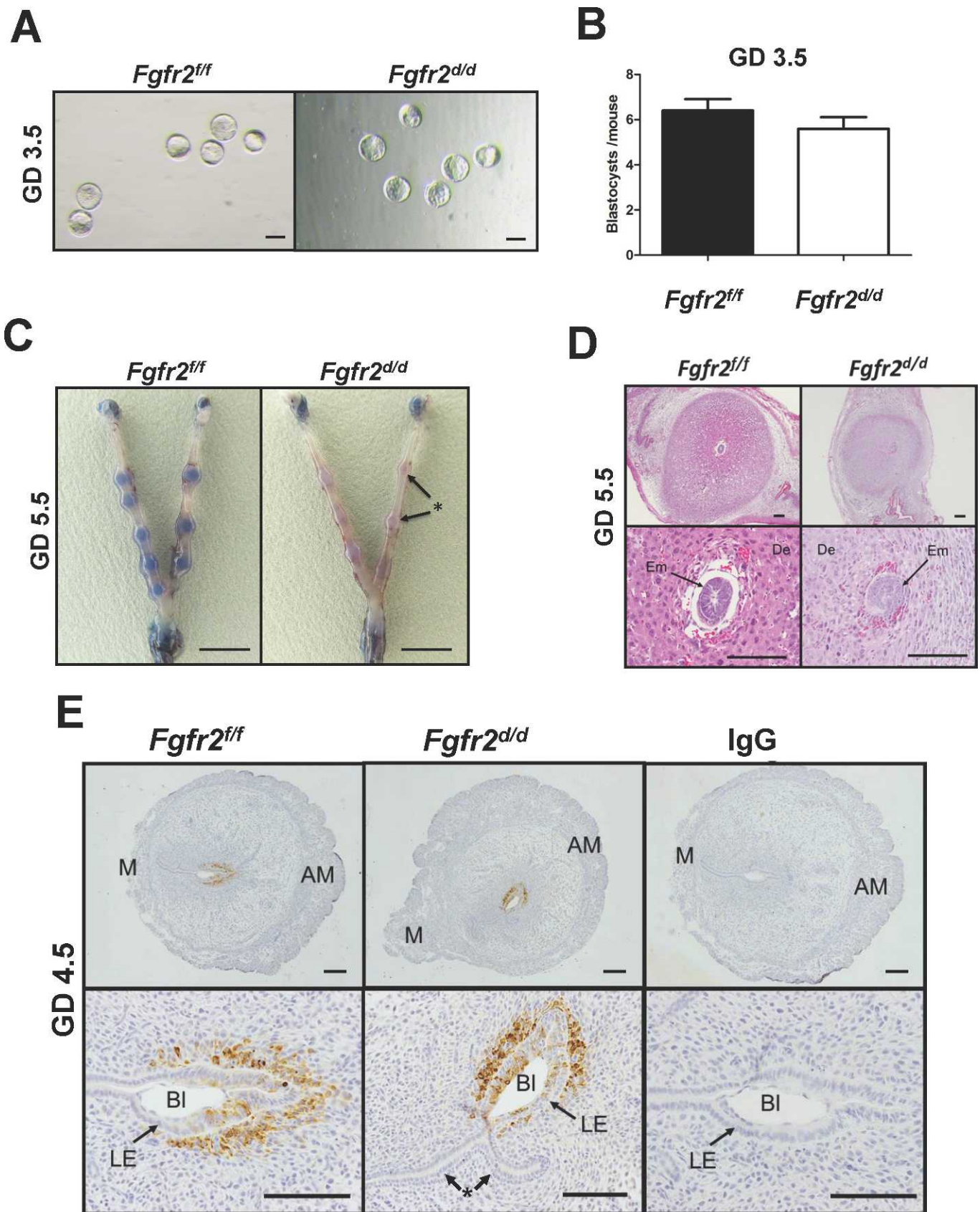
Article 7

FIG. 4. Pregnancy defects in conditional *Fgfr2* mutant mice. **A**, **B**) Blastocysts recovered from adult primiparous *Fgfr2^{f/f}* and *Fgfr2^{d/d}* mice on Gestational Day (GD) 3.5. The error bar denotes standard error of the mean number of embryos (n = 5 mice/genotype). Bar = 100 µm. **C**) Implantation sites in the *Fgfr2^{f/f}* and *Fgfr2^{d/d}* uterus on GD 5.5 revealed by intravenous injection of a macromolecular blue dye. The *Fgfr2^{d/d}* mutant uteri possess implantation sites (asterisks) that are not blue dye positive as observed in *Fgfr2^{f/f}* control uteri (n = 6 mice/genotype). **D**) Histological analysis of implantation sites on GD 5.5. Sections of the uterus were stained with hematoxylin and eosin. De, decidualized stromal cells; Em, embryo. Bar = 100 µm. **E**) Immunohistochemical

*Fgfr2^{f/f}* than *Fgfr2^{d/d}* females. Indeed, the *Fgfr2^{d/d}* females displayed a pronounced parity-dependent decline in fertility (Fig. 3). Interestingly, the *Fgfr2^{d/d}* females have lower number of pups in the first and subsequent parities (genotype × parity, $P < 0.05$). Thus, postnatal conditional loss of *Fgfr2* in the mouse uterus compromises female fertility.

In order to elucidate the nature of the fertility defect in *Fgfr2^{d/d}* mice, *Fgfr2^{f/f}* and *Fgfr2^{d/d}* mice were mated to males of proven fertility. Both *Fgfr2^{f/f}* and *Fgfr2^{d/d}* mice displayed normal mating behavior as determined by the presence of postcopulatory vaginal plug (data not shown). Next, nulliparous 8 wk-old *Fgfr2^{f/f}* and *Fgfr2^{d/d}* mice were mated, and uteri were flushed on GD 3.5 to quantify blastocyst number and morphology. Blastocysts of normal morphology and number were recovered from the uteri of *Fgfr2^{d/d}* mice on Day 3.5 postmating (Fig. 4, A and B). Embryo implantation was assessed in nulliparous *Fgfr2^{f/f}* and *Fgfr2^{d/d}* mice on GD 5.5 by intravenous injection of a macromolecular blue dye that accumulates at sites of increased vascular permeability and can be used to visualize the location of embryo implantation [38]. Implantation sites were easily discernible on GD 5.5 in the uteri of control *Fgfr2^{f/f}* mice, but not in *Fgfr2^{d/d}* mice (Fig. 4C). Of note, distinct bulges in the uterus were consistently observed in *Fgfr2^{d/d}* mice on GD 5.5, which is characteristic of the implanting embryos, but those sites contained little if any accumulation of macromolecular blue dye. Histologically, the uteri of *Fgfr2^{d/d}* mutant mice contained implanted embryos and polyploid decidualized stromal cells (Fig. 4D). Next, nulliparous control and mutant mice were mated and analyzed on GD 4.5 (Fig. 4E). In both *Fgfr2^{f/f}* and *Fgfr2^{d/d}* mice, implantation sites contained evidence of uterine luminal closure with a blastocyst apposed to the LE within the implantation chamber. Interestingly, an uncharacteristic bilaminar or stratified LE was observed in the uteri of *Fgfr2^{d/d}* mice but not *Fgfr2^{f/f}* mice (Fig. 4E). Prostaglandin endoperoxide synthase two (PTGS2) is expressed in the decidualizing stromal cells at the site of blastocyst attachment and is a marker of appropriate embryo implantation in mice [39]. In both *Fgfr2^{f/f}* and *Fgfr2^{d/d}* mice, PTGS2 was present in the decidualizing stromal cells adjacent to the implanting blastocyst (Fig. 4E).

*Conditional Deletion of FGFR2 Elicits Epithelial Stratification in the Adult Uterus*

As illustrated in Figure 5A, no difference in histoarchitecture of the ovary, oviduct, cervix, or vagina was found in *Fgfr2^{f/f}* and *Fgfr2^{d/d}* mice. With the exception of the LE, the uterus was not different in control and mutant mice (Fig. 5B). In contrast to the single layer of columnar LE observed in *Fgfr2^{f/f}* uteri, uteri from *Fgfr2^{d/d}* mice contained a second cell layer underneath the columnar LE, indicative of a stratified type of epithelium containing basal cells. However, the endometrial GE remained simple and cuboidal in nature and histologically normal in *Fgfr2^{d/d}* uteri. Of note, the stratified regions of epithelium were intermittent and not present throughout the entire LE of the uterus of nulliparous *Fgfr2^{d/d}* mutant mice. Real-time PCR analysis revealed that the uteri of *Fgfr2^{d/d}* mice had considerably higher ($P < 0.05$) levels of *keratin 14* (*Krt14*) mRNA (72-fold increase) and *small proline-rich protein 2b* (*Sprr2b*) mRNA (7-fold increase) as compared

to control uteri (Fig. 5C). Both KRT14 and SPRR2B are abundantly expressed in stratified squamous types of epithelia, such as the vagina [40, 41], but are not normally abundant in the epithelium of the uterus.

To better understand the nature of LE stratification in the *Fgfr2^{d/d}* mutant mice, expression of transformation-related protein 63 (TRP63) and KRT14, two basal cell markers [42], were analyzed in the neonatal and adult uterus (Fig. 6). Both TRP63- and KRT14-positive cells were present in layer of LE in the uterus of *Fgfr2^{d/d}* mutant but not in *Fgfr2^{f/f}* uteri. The KRT14- and TRP63-positive cells were not observed in *Fgfr2^{f/f}* and *Fgfr2^{d/d}* uteri on PD 5, but were observed by PD 12 only in the LE of *Fgfr2^{d/d}* mutant mice. Both *Fgfr2^{f/f}* and *Fgfr2^{d/d}* uteri contained histologically normal uterine glands that were lined with single-layered cuboidal GE.

In the neonatal and adult uterus, FOXA2 is expressed solely in GE and is not present in other cell types [31, 35–37]. Immunoreactive FOXA2 was present in the nuclei of GE cells in the neonatal and adult uterus of both *Fgfr2^{f/f}* and *Fgfr2^{d/d}* mice (Fig. 7A). Surprisingly, FOXA2-positive cells were clearly present in the stratified LE of the *Fgfr2^{d/d}* mutant uterus. In contrast to TRP63 and KRT14, FOXA2 protein was not present in the basal cells and was in the upper layer of cells within the stratified LE, particularly in the adult GD 3.5 uterus. Real-time PCR analysis revealed that the uteri of *Fgfr2^{d/d}* mice contained elevated ($P < 0.01$) levels of *Foxa2* mRNA (2-fold increase) as compared to control uteri (Fig. 7B).

## DISCUSSION

The *Pgr^{Cre}* mouse was used in this study to conditionally delete *Fgfr2* in the female reproductive tract after birth because global *Fgfr2* knockout mice are embryonic lethal. This approach resulted in substantial decreases in uterine *Fgfr2IIIb* mRNA levels on PD 5 and thereafter. Although *Fgfr2IIIc* mRNA levels were not different in the uterus of control and mutant mice on PD 5, they were lower in mutant mice on PD 12 and 28. The efficiency of deletion in the two *Fgfr2* isoforms may be due to differences in cell-specific expression of the different *Fgfr2* isoforms as well as Cre activity in the uterus due to *Pgr* expression. In the neonatal mouse uterus, *Pgr* expression is initiated in the uterine LE immediately after birth, but PGR protein is not present in the stroma until PD 6 [8]. The FGFR2 and its ligands are implicated in epithelial morphogenesis in numerous organs, including the mammary gland, prostate, lung, and kidney [16–20]. However, uteri of conditional *Fgfr2* deficient mice developed endometrial glands by PD 12 that were histoarchitecturally normal and not different from control mice. These results support the idea that FGFR2 does not have a biological role in endometrial GE differentiation from the LE and subsequent GE development in the neonatal mouse uterus. In contrast, FGFR2 clearly has a biological role in maintaining the identity and integrity of the LE of the uterus.

The development of a stratified LE with basal cells in the postnatal *Fgfr2* mutant uterus was an unexpected finding that supports a role for FGFR2 and its ligands in regulating the differentiated phenotype of uterine LE. In the adult mouse, several FGFs act as paracrine mediators of the mitogenic effects of estrogen on the LE of the uterus [9]. A recent study

localization of PTGS2 in *Fgfr2^{f/f}* and *Fgfr2^{d/d}* uteri on GD 4.5 (n = 4 mice/genotype). Sections were counterstained with hematoxylin after protein localization. Note the presence of a bilaminar or stratified LE adjacent to the embryo implantation site in the *Fgfr2^{d/d}* uterus denoted by an asterisk (*). AM, antimesometrial; Bl, blastocyst; LE, luminal epithelium; M, mesometrial. Bar = 100 μm.
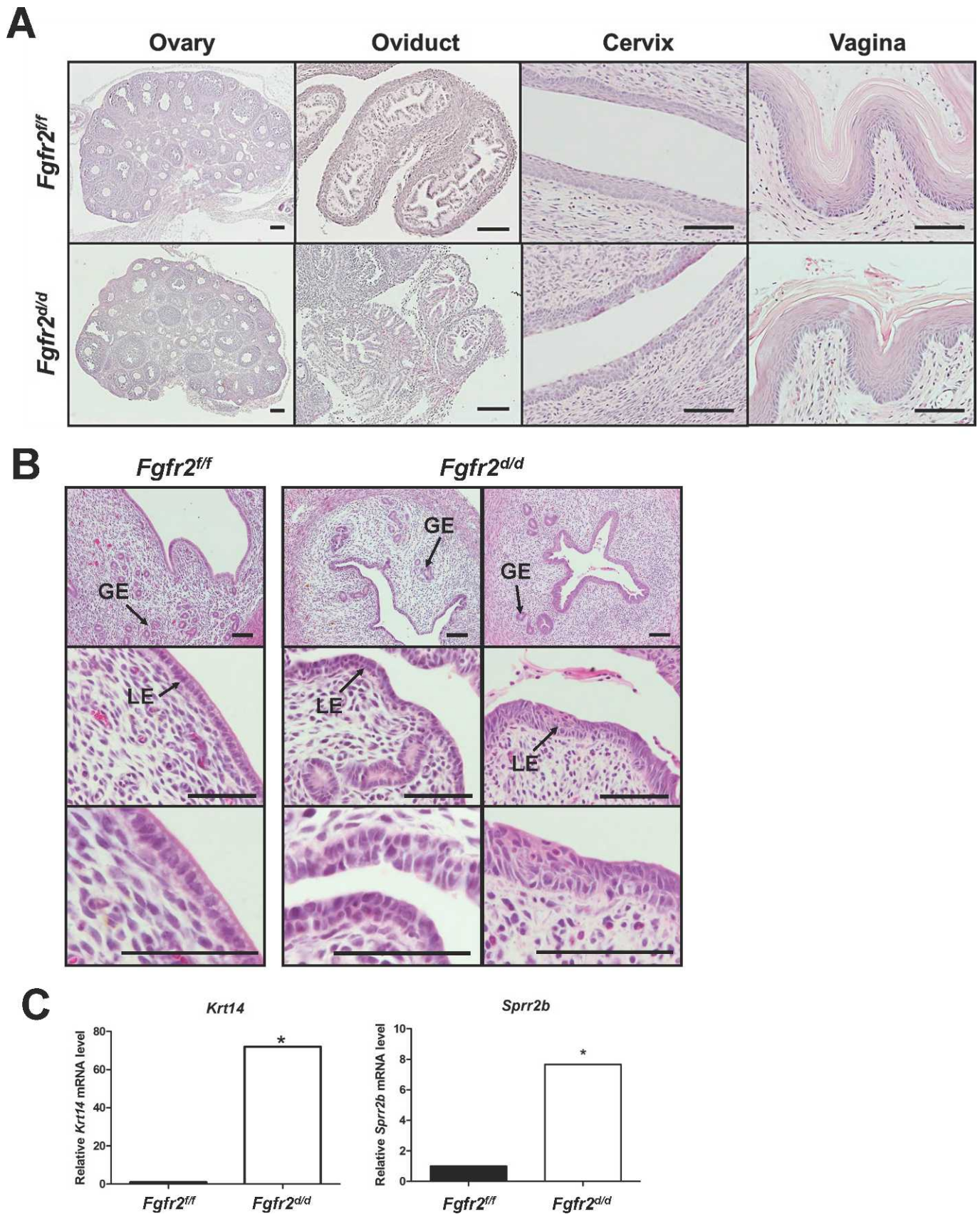
FIG. 5. Analysis of the female reproductive tract of adult $Fgfr2^{f/f}$ and $Fgfr2^{d/d}$ mice. **A**) Histology of the ovary, oviduct, cervix, and vagina of nulliparous $Fgfr2^{f/f}$ and $Fgfr2^{d/d}$ mice. Reproductive tract tissue sections were stained with hematoxylin and eosin. Bar = 100 μm. **B**) Histological examination of the uteri collected on Gestational Day (GD) 3.5 from nulliparous $Fgfr2^{f/f}$ (on the left) and $Fgfr2^{d/d}$ mice (middle and right images). Sections of uteri were
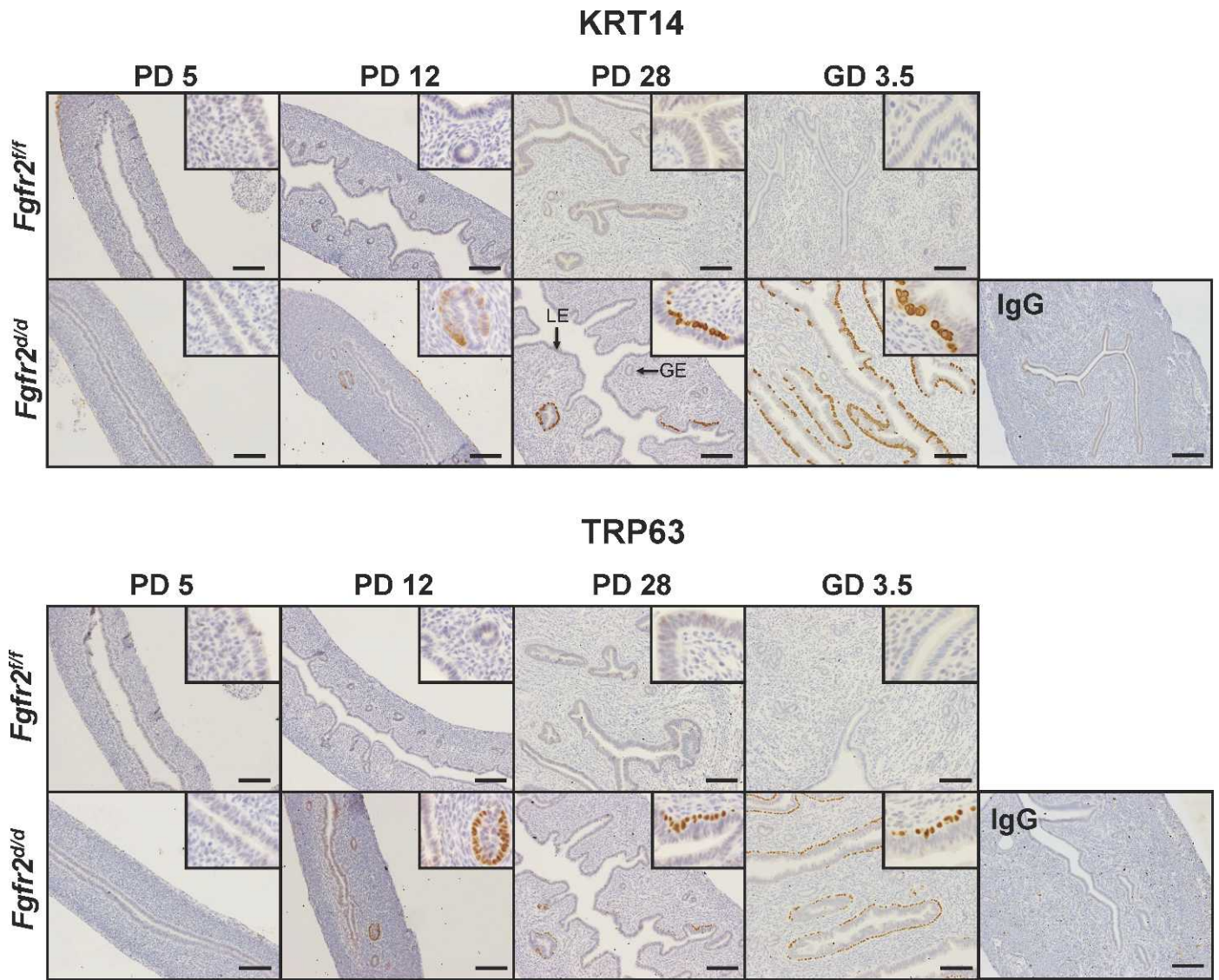
## KRT14



## TRP63



FIG. 6. TRP63 and KRT14 in the uteri of *Fgfr2*^f/f^ and *Fgfr2*^d/d^ mice. Sections of neonatal and adult mice were briefly counterstained with hematoxylin after immunohistochemical localization of TRP63 or KRT14 protein (n = 4 mice/day/genotype). Note the presence of TRP63- and KRT14-positive basal cells in the stratified LE in uteri of *Fgfr2*^d/d^ mice. GD, gestational day; GE, glandular epithelium; LE, luminal epithelium; PD, postnatal day. Bar = 100 μm. Magnification of insets ×80.

proposed that FGF signaling is involved in vaginal and uterine epithelial differentiation in neonatal mice [21]. Specifically, it was hypothesized that epithelium-derived FGF9 stimulates uterus-type epithelial differentiation through FGFR2IIIc in an autocrine manner. Indeed, FGF9 inhibited the expression of *Krt14* whereas the inactivation of FGF9 by a specific antibody induced the expression of *Krt14* in the vaginal epithelium, suggesting that the FGF9 inhibits epithelial stratification [21]. Our findings support the hypothesis that FGF9-FGFR2IIIc signaling in the uterine epithelium prevents epithelial stratification because *Fgfr2* deficiency triggered stratification in the LE of the uterus. Another possible mechanism for epithelial stratification is mesenchymal-to-epithelial transition. The epithelium of the lower portion of the Müllerian duct expresses

TRP63 on Embryonic Day 18, and TRP63-positive cells express KRT14 on PD 2 [8, 43]. The expression of *Trp63* is essential for the stratified squamous differentiation because the epithelium of the Müllerian vagina in *Trp63* null mice formed a uterus-like layer of columnar epithelium [43]. In the normal uterus, FOXA2 is expressed solely in the GE cells of the uterus [9, 31, 36, 37, 44, 45] and was present in the nuclei of endometrial glands of *Fgfr2*^d/d^ mutant mice. Indeed, FOXA2 protein is present in the nuclei of the upper, nonbasal cell layer of the stratified vaginal epithelia in the embryonic, neonatal, and adult mouse (Filant and Spencer, unpublished results). The biological role, if any, of FOXA2 in the vaginal epithelium is not known, but FOXA2 regulates the proliferation of many different cell types [46–48]. Epithelial stratification is also

stained with hematoxylin and eosin. Note the presence of stratified LE in the uterus of *Fgfr2*^d/d^ mutant mice. LE, luminal epithelium; GE, glandular epithelium. Bar = 100 μm. **C**) *Krt14* and *Sprr2b* mRNA in the uterus of *Fgfr2*^f/f^ and *Fgfr2*^d/d^ mice on GD 3.5. The relative mRNA levels of *Krt14* and *Sprr2b* were measured in the GD 3.5 uterus by real-time RT-PCR. Data are presented as fold change relative to the mRNA level in uteri from *Fgfr2*^f/f^ mice (n = 4 mice/genotype).
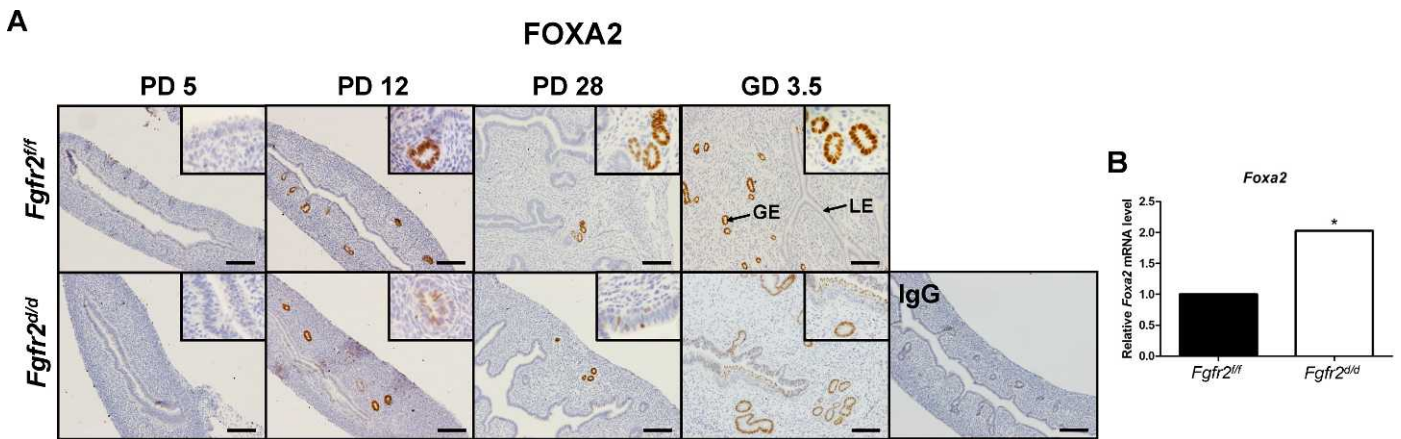
**A** FOXA2

**B** *Foxa2*

FIG. 7. FOXA2 in uteri of *Fgfr2$^{f/f}$* and *Fgfr2$^{d/d}$* mice. **A**) Sections of neonatal and adult mice were briefly counterstained with hematoxylin after immunohistochemical localization of FOXA2 protein (n = 4 mice/day/genotype). Note the presence of FOXA2-positive cells in the upper cells of the stratified LE in uteri of *Fgfr2$^{d/d}$* mice. GD, gestational day; GE, glandular epithelium; LE, luminal epithelium; PD, postnatal day. Bar = 100 μm. Magnification of insets ×80. **B**) *Foxa2* mRNA in the uterus of control and mutant mice on GD 3.5. The relative mRNA levels of *Foxa2* were measured in the GD 3.5 uterus of nulliparous *Fgfr2$^{f/f}$* and *Fgfr2$^{d/d}$* mice by real-time RT-PCR. Data are presented as fold change relative to the mRNA level in uteri from *Fgfr2$^{f/f}$* mice (n = 4 mice/genotype). Effects of genotype are indicated by an asterisk ($P < 0.05$).

observed in conditional mutants of *Wnt4* (*Pgre$^{Cre}$;Wnt4$^{f/f}$*) [44]. Squamous cell carcinoma accounts for a small portion of endometrial cancers and is thought to arise from the cervix [49]. However, these lesions may arise from the uterus itself based on this study and others [8, 44]. Patients with this type of cancer only survive an average of 40 mo, even after treatment, demonstrating a need to better understand this disease [49]. Therefore, the *Fgfr2* conditional mouse model may be useful to understand the origin of uterine squamous cell carcinoma.

The conditional *Fgfr2* mutant mice were initially subfertile and then became infertile with increasing parity. The subfertility and infertility do not appear to involve dysfunction of the ovary or oviduct because their histology and function were not different between nulliparous control and *Fgfr2$^{d/d}$* mutant mice. Further, no difference in blastocyst morphology or number was found on GD 3.5. Although unlikely, one possibility is faulty oocyte development (e.g., meiosis) during folliculogenesis may allow for embryo attachment and implantation, but then results in postimplantation embryonic demise. At term, fetal survival was only 37% in first parity *Fgfr2$^{d/d}$* mutant mice, even though they yielded normal numbers of blastocysts on GD 3.5. On GD 4.5 in the *Fgfr2$^{d/d}$* uterus, embryo implantation sites were histologically normal with PTGS2 in the decidualizing stromal cells adjacent to the blastocysts attached to the LE. However, implantation was abnormal on GD 5.5 in the *Fgfr2$^{d/d}$* mutant mice based on vascular permeability as detected using intravenous injection of macromolecular blue dye. An increase in vascular permeability and angiogenesis are critical for successful implantation, decidualization, and placentation (for a review, see [50]). A localized increase in vascular permeability is the first conspicuous sign of blastocyst attachment, and it can be readily visualized by intravenous injection of a macromolecular blue dye [38]. The implantation sites in *Fgfr2$^{d/d}$* mice accumulated observably much less dye than implantation sites in control mice on GD 5.5. An increase in microvascular permeability is thought to facilitate growth and differentiation of the endometrium in preparation for implantation and pregnancy [51]. Vascular endothelial growth factor (VEGF) is proposed as a principal mediator of estrogen-induced increase in uterine vascular permeability [51]. The action of VEGF on endothelial cells is mediated by VEGF receptors FLT1 and KDR (for a review, see [52]). Interestingly, FGF

signaling controls endothelial cell responsiveness to VEGF by modulation of KDR expression [53], and FGFR2 regulates endothelial cell migration [54]. In the present study, FGF signaling was disrupted via conditional deletion of *Fgfr2* in all the PGR-expressing cells, and PGR is expressed by endothelial cells [55]. Thus, these results support the idea that ablation of FGFR2 potentially alters VEGF signaling in endothelial cells, thereby impairing vascular permeability in the uterus. It is tempting to speculate that progressive stratification of the entire LE occurs with increasing parity and contributes to the complete infertility observed in multiparous *Fgfr2* mutant mice. The presence of stratified LE together with the impairment in vascular permeability could affect uterine receptivity and stromal decidualization in *Fgfr2$^{d/d}$* uteri. Further studies are necessary to reveal the precise cellular and molecular mechanisms contributing to embryonic loss in conditional *Fgfr2* mutant mice.

In summary, conditional ablation of FGFR2 after birth in the mouse uterus resulted in the abnormal appearance of basal cells in the LE, stratification of the LE, and subfertility that progressed to infertility. These findings demonstrate a critical role for FGFR2 in proper postnatal uterine development as well as normal uterine function. Further examination into FGFR2 and its signaling pathways could provide insight into pathways that are deregulated during endometrial diseases, such as endometrial cancer. Accordingly, this mouse model should be useful to determine age-related effects on fertility and basic mechanisms important for uterine receptivity and implantation as well as uterine regeneration and epithelial homeostasis and integrity.

## REFERENCES

1. Cunha GR. Epithelial-stromal interactions in development of the urogenital tract. Int Rev Cytol 1976; 47:137–194.
2. Cunha GR. Stromal induction and specification of morphogenesis and cytodifferentiation of the epithelia of the Mullerian ducts and urogenital sinus during development of the uterus and vagina in mice. J Exp Zool 1976; 196:361–370.
3. Sharpe PM, Ferguson MW. Mesenchymal influences on epithelial differentiation in developing systems. J Cell Sci Suppl 1988; 10:195–230.
4. Cunha GR, Chung LW, Shannon JM, Taguchi O, Fujii H. Hormone-induced morphogenesis and growth: role of mesenchymal-epithelial interactions. Recent Prog Horm Res 1983; 39:559–598.
5. Cunha GR, Young P, Brody JR. Role of uterine epithelium in the

development of myometrial smooth muscle cells. Biol Reprod 1989; 40: 861–871.

6. Kurita T, Cooke PS, Cunha GR. Epithelial-stromal tissue interaction in paramesonephric (Mullerian) epithelial differentiation. Dev Biol 2001; 240:194–211.

7. Brody JR, Cunha GR. Histologic, morphometric, and immunocytochemical analysis of myometrial development in rats and mice: I. Normal development. Am J Anat 1989; 186:1–20.

8. Kurita T. Normal and abnormal epithelial differentiation in the female reproductive tract. Differentiation 2011; 82:117–126.

9. Li Q, Kannan A, DeMayo FJ, Lydon JP, Cooke PS, Yamagishi H, Srivastava D, Bagchi MK, Bagchi IC. The antiproliferative action of progesterone in uterine epithelium is mediated by Hand2. Science 2011; 331:912–916.

10. Spencer TE, Dunlap KA, Filant J. Comparative developmental biology of the uterus: insights into mechanisms and developmental disruption. Mol Cell Endocrinol 2012; 354:34–53.

11. Hayashi K, Yoshioka S, Reardon SN, Rucker EB III, Spencer TE, Demayo FJ, Lydon JP, Maclean JA II. WNTs in the neonatal mouse uterus: potential regulation of endometrial gland development. Biol Reprod 2011; 84:308–319.

12. Raines AM, Adam M, Magella B, Meyer SE, Grimes HL, Dey SK, Potter SS. Recombineering-based dissection of flanking and paralogous Hox gene functions in mouse reproductive tracts. Development 2013; 140: 2942–2952.

13. Rubel CA, Jeong JW, Tsai SY, Lydon JP, Demayo FJ. Epithelial-stromal interaction and progesterone receptors in the mouse uterus. Semin Reprod Med 2010; 28:27–35.

14. Zhang S, Lin H, Kong S, Wang S, Wang H, Wang H, Armant DR. Physiological and molecular determinants of embryo implantation. Mol Aspects Med 2013; 34:939–980.

15. Cha J, Sun X, Dey SK. Mechanisms of implantation: strategies for successful pregnancy. Nat Med 2012; 18:1754–1767.

16. Celli G, LaRochelle WJ, Mackem S, Sharp R, Merlino G. Soluble dominant-negative receptor uncovers essential roles for fibroblast growth factors in multi-organ induction and patterning. EMBO J 1998; 17: 1642–1655.

17. De Moerlooze L, Spencer-Dene B, Revest JM, Hajihosseini M, Rosewell I, Dickson C. An important role for the IIIb isoform of fibroblast growth factor receptor 2 (FGFR2) in mesenchymal-epithelial signalling during mouse organogenesis. Development 2000; 127:483–492.

18. Abler LL, Mansour SL, Sun X. Conditional gene inactivation reveals roles for Fgf10 and Fgfr2 in establishing a normal pattern of epithelial branching in the mouse lung. Dev Dyn 2009; 238:1999–2013.

19. Steinberg Z, Myers C, Heim VM, Lathrop CA, Rebustini IT, Stewart JS, Larsen M, Hoffman MP. FGFR2b signaling regulates ex vivo submandibular gland epithelial cell proliferation and branching morphogenesis. Development 2005; 132:1223–1234.

20. Jackson D, Bresnick J, Dickson C. A role for fibroblast growth factor signaling in the lobuloalveolar development of the mammary gland. J Mammary Gland Biol Neoplasia 1997; 2:385–392.

21. Nakajima T, Hayashi S, Iguchi T, Sato T. The role of fibroblast growth factors on the differentiation of vaginal epithelium of neonatal mice. Differentiation 2011; 82:28–37.

22. Hom YK, Young P, Thomson AA, Cunha GR. Keratinocyte growth factor injected into female mouse neonates stimulates uterine and vaginal epithelial growth. Endocrinology 1998; 139:3772–3779.

23. Itoh N, Ornitz DM. Fibroblast growth factors: from molecular evolution to roles in development, metabolism and disease. J Biochem 2011; 149: 121–130.

24. Bellusci S, Grindley J, Emoto H, Itoh N, Hogan BL. Fibroblast growth factor 10 (FGF10) and branching morphogenesis in the embryonic mouse lung. Development 1997; 124:4867–4878.

25. Finch PW, Cunha GR, Rubin JS, Wong J, Ron D. Pattern of keratinocyte growth factor and keratinocyte growth factor receptor expression during mouse fetal development suggests a role in mediating morphogenetic mesenchymal-epithelial interactions. Dev Dyn 1995; 203:223–240.

26. Ornitz DM, Xu J, Colvin JS, McEwen DG, MacArthur CA, Coulier F, Gao G, Goldfarb M. Receptor specificity of the fibroblast growth factor family. J Biol Chem 1996; 271:15292–15297.

27. Orr-Urtreger A, Bedford MT, Burakova T, Arman E, Zimmer Y, Yayon A, Givol D, Lonai P. Developmental localization of the splicing alternatives of fibroblast growth factor receptor-2 (FGFR2). Dev Biol 1993; 158: 475–486.

28. Arman E, Haffner-Krausz R, Chen Y, Heath JK, Lonai P. Targeted disruption of fibroblast growth factor (FGF) receptor 2 suggests a role for FGF signaling in pregastrulation mammalian development. Proc Natl Acad Sci U S A 1998; 95:5082–5087.

29. Soyal SM, Mukherjee A, Lee KY, Li J, Li H, DeMayo FJ, Lydon JP. Cre-mediated recombination in cell lineages that express the progesterone receptor. Genesis 2005; 41:58–66.

30. Yu K, Xu J, Liu Z, Sosic D, Shao J, Olson EN, Towler DA, Ornitz DM. Conditional inactivation of FGF receptor 2 reveals an essential role for FGF signaling in the regulation of osteoblast function and bone growth. Development 2003; 130:3063–3074.

31. Dunlap KA, Filant J, Hayashi K, Rucker EB III, Song G, Deng JM, Behringer RR, DeMayo FJ, Lydon J, Jeong JW, Spencer TE. Postnatal deletion of wnt7a inhibits uterine gland morphogenesis and compromises adult fertility in mice. Biol Reprod 2011; 85:386–396.

32. Revest JM, Spencer-Dene B, Kerr K, De Moerlooze L, Rosewell I, Dickson C. Fibroblast growth factor receptor 2-IIIb acts upstream of Shh and Fgf4 and is required for limb bud maintenance but not for the induction of Fgf8, Fgf10, Msx1, or Bmp4. Dev Biol 2001; 231:47–62.

33. Eswarakumar VP, Monsonego-Ornan E, Pines M, Antonopoulou I, Morriss-Kay GM, Lonai P. The IIIc alternative of Fgfr2 is a positive regulator of bone formation. Development 2002; 129:3783–3793.

34. Franco HL, Jeong JW, Tsai SY, Lydon JP, DeMayo FJ. In vivo analysis of progesterone receptor action in the uterus during embryo implantation. Semin Cell Dev Biol 2008; 19:178–186.

35. Jeong JW, Kwak I, Lee KY, Kim TH, Large MJ, Stewart CL, Kaestner KH, Lydon JP, DeMayo FJ. Foxa2 is essential for mouse endometrial gland development and fertility. Biol Reprod 2010; 83:396–403.

36. Filant J, Spencer TE. Endometrial glands are essential for blastocyst implantation and decidualization in the mouse uterus. Biol Reprod 2013; 88:93.

37. Filant J, Zhou H, Spencer TE. Progesterone inhibits uterine gland development in the neonatal mouse uterus. Biol Reprod 2012; 86:146.

38. Psychoyos A. Hormonal control of ovoimplantation. Vitam Horm 1973; 31:201–256.

39. Chakraborty I, Das SK, Wang J, Dey SK. Developmental expression of the cyclo-oxygenase-1 and cyclo-oxygenase-2 genes in the peri-implantation mouse uterus and their differential regulation by the blastocyst and ovarian steroids. J Mol Endocrinol 1996; 16:107–122.

40. Gimenez-Conti IB, Lynch M, Roop D, Bhowmik S, Majeski P, Conti CJ. Expression of keratins in mouse vaginal epithelium. Differentiation 1994; 56:143–151.

41. Tan YF, Sun XY, Li FX, Tang S, Piao YS, Wang YL. Gene expression pattern and hormonal regulation of small proline-rich protein 2 family members in the female mouse reproductive system during the estrous cycle and pregnancy. Reprod Nutr Dev 2006; 46:641–655.

42. Koster MI, Roop DR. Mechanisms regulating epithelial stratification. Annu Rev Cell Dev Biol 2007; 23:93–113.

43. Kurita T, Mills AA, Cunha GR. Roles of p63 in the diethylstilbestrol-induced cervicovaginal adenosis. Development 2004; 131:1639–1649.

44. Franco HL, Dai D, Lee KY, Rubel CA, Roop D, Boerboom D, Jeong JW, Lydon JP, Bagchi IC, Bagchi MK, DeMayo FJ. WNT4 is a key regulator of normal postnatal uterine development and progesterone signaling during embryo implantation and decidualization in the mouse. FASEB J 2011; 25:1176–1187.

45. Besnard V, Wert SE, Hull WM, Whitsett JA. Immunohistochemical localization of Foxa1 and Foxa2 in mouse embryos and adult tissues. Gene Expr Patterns 2004; 5:193–208.

46. Wan H, Kaestner KH, Ang SL, Ikegami M, Finkelman FD, Stahlman MT, Fulkerson PC, Rothenberg ME, Whitsett JA. Foxa2 regulates alveolarization and goblet cell hyperplasia. Development 2004; 131:953–964.

47. Li Z, White P, Tuteja G, Rubins N, Sackett S, Kaestner KH. Foxa1 and Foxa2 regulate bile duct development in mice. J Clin Invest 2009; 119: 1537–1545.

48. Villacorte M, Suzuki K, Hirasawa A, Ohkawa Y, Suyama M, Maruyama T, Aoki D, Ogino Y, Miyagawa S, Terabayashi T, Tomooka Y, Nakagata N, et al. beta-Catenin signaling regulates Foxa2 expression during endometrial hyperplasia formation. Oncogene 2013; 32:3477–3482.

49. Mendivil A, Schuler KM, Gehrig PA. Non-endometrioid adenocarcinoma of the uterine corpus: a review of selected histological subtypes. Cancer Control 2009; 16:46–52.

50. Dey SK, Lim H, Das SK, Reese J, Paria BC, Daikoku T, Wang H. Molecular cues to implantation. Endocr Rev 2004; 25:341–373.

51. Rockwell LC, Pillai S, Olson CE, Koos RD. Inhibition of vascular endothelial growth factor/vascular permeability factor action blocks estrogen-induced uterine edema and implantation in rodents. Biol Reprod 2002; 67:1804–1810.

52. Olsson AK, Dimberg A, Kreuger J, Claesson-Welsh L. VEGF receptor

signalling—in control of vascular function. Nat Rev Mol Cell Biol 2006; 7:359–371.

53. Murakami M, Nguyen LT, Zhuang ZW, Moodie KL, Carmeliet P, Stan RV, Simons M. The FGF system has a key role in regulating vascular integrity. J Clin Invest 2008; 118:3355–3366.

54. Nakamura T, Mochizuki Y, Kanetake H, Kanda S. Signals via FGF receptor 2 regulate migration of endothelial cells. Biochem Biophys Res Commun 2001; 289:801–806.

55. Vazquez F, Rodriguez-Manzaneque JC, Lydon JP, Edwards DP, O'Malley BW, Iruela-Arispe ML. Progesterone regulates proliferation of endothelial cells. J Biol Chem 1999; 274:2185–2192.